Tetrahedron 65 (2009) 4742–4750

Contents lists available at ScienceDirect

Tetrahedron

journal homepage: www.elsevier.com/locate/tet

Investigation of electrochemically induced Michael addition reactions. Oxidation of some dihydroxybenzene derivatives in the presence of azide ion

Davood Nematollahi *, Hosain Khoshsafar

Faculty of Chemistry, Bu-Ali-Sina University, P.O. Box 65174, Hamadan, Iran

ARTICLE INFO

Article history:
Received 22 January 2009
Received in revised form 18 March 2009
Accepted 2 April 2009
Available online 10 April 2009

ABSTRACT

In aqueous solution containing azide ion as a nucleophile, electrochemical oxidation of hydroquinone and some dihydroxybenzoic acids have been studied using cyclic voltammetry and controlled-potential coulometry. The voltammetric data show that electrochemically generated *para* and *ortho*-benzoquinones participate in Michael addition reactions with azide ions to form the corresponding diazido or diaminobenzoquinones. In this work, we have proposed various mechanisms for the electrode process and we report an efficient and one-pot method for the synthesis of 2,5-diazido-1,4-benzoquinone, 2,5-diamino-1,4-benzoquinone, 4,5-diamino-1,2-benzoquinone, and 2,3-diamino-5,6-dioxocyclohexa-1,3-dienecarboxylic acid based on the Michael reaction of electrochemically generated *ortho* and *para*-benzoquinones with azide ion in an undivided cell using an environmentally friendly reagent-less method in ambient conditions. An estimation of the observed homogeneous rate constant (k_{obs}) of the reaction of electrochemically generated *para*-benzoquinone with azide ion by the digital simulation method is also presented.

1. Introduction

The conjugate addition reaction of azides to α,β-unsaturated carbonyl compounds is a useful method in synthetic organic chemistry, providing efficient access to a variety of natural products or compounds with pronounced biological activity.[1,2] Also, the chemistry of azides has been the subject of many investigations because of their importance in preparative heterocyclic chemistry.[3] In this context, azidoquinones constitute a synthetically versatile and readily available class of compounds. Depending upon their substitution pattern and the reaction conditions, a variety of very specific and high yielding transformations can be accomplished.[4–14] On the other hand, amino derivatives of quinones are important building blocks in the synthesis of a variety of natural products, medicinal compounds[15–21] with antitumor and antimalarial activities.[22,23] The importance of these compounds has motivated us to study the electrochemical oxidation of catechol in the presence of azide ion and to synthesize 4,5-diamino-*o*-benzoquinone.[24] In a continuation of our efforts to develop the synthesis of azido and amino derivatives of quinones and to study the kinetics of the reaction of quinones with azide ions, and following our experience in electrochemical synthesis of organic compounds based on the oxidation of catechols and hydroquinones in the presence of nucleophiles,[25–32] herein we wish to describe a one-pot and straightforward protocol for the synthesis of some diazido and diaminobenzoquinones (*ortho* and *para*) via electrochemical oxidation of hydroquinone and some dihydroxybenzoic acids in the presence of azide ions. The reaction proceeds in a single step with an environmentally friendly reagent-less method in aqueous solution with high atom economy in ambient conditions in an undivided cell using a graphite electrode. Furthermore, the observed homogeneous rate constant (k_{obs}) of the intramolecular reaction of electrochemically generated *para*-benzoquinones with azide ions has been estimated by the digital simulation of the cyclic voltammograms.

2. Results and discussion

2.1. Electrochemical oxidation of hydroquinone

Figure 1, curve a, shows the voltammetric curve obtained for the oxidation of hydroquinone (**1**) (1 mM) in water containing phosphate buffer (c=0.2 M, pH=6.0) at a glassy carbon electrode. In the studied potential range, a well-defined voltammetric curve is obtained that has an anodic (A_1) and the corresponding cathodic (C_1) peaks. These peaks correspond to the oxidation of hydroquinone (**1**) to *p*-benzoquinone (**1ox**) and vice versa within a reversible two-electron process.[26,29,31] The oxidation of hydroquinone (**1**) in the presence of azide ion as a nucleophile was studied in some detail. Figure 1, curve b shows the cyclic voltammogram obtained

* Corresponding author. Tel.: +98 811 8282807; fax: +98 811 8257407.
E-mail address: nemat@basu.ac.ir (D. Nematollahi).

0040-4020/$ – see front matter © 2009 Elsevier Ltd. All rights reserved.
doi:10.1016/j.tet.2009.04.015

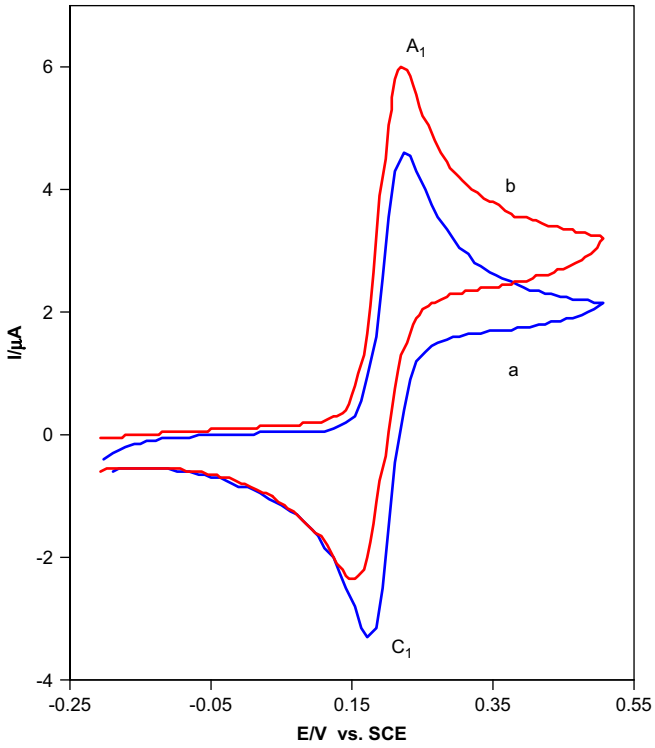

Figure 1. Cyclic voltammograms of 1 mM hydroquinone (**1**): (a) in the absence (b) in the presence of 30 mM of azide ion in water containing phosphate buffer (c=0.2 M, pH=6.0) at glassy carbon electrode. Scan rate: 10 mV s^{-1}; t=25±1 °C.

for a 1 mM solution of **1** in the presence of 30 mM of azide ion. Under these conditions, the voltammogram exhibits anodic and cathodic peaks A_1 and C_1, respectively. The comparison of A_1 and C_1 peaks in the absence and presence of azide ion shows an increase in peak A_1 and a decrease in peak C_1. This indicates the reactivity of electrochemically generated *p*-benzoquinone toward azide ion. The existence of a subsequent chemical reaction is supported by the following evidence: (a) increasing of peak A_1 current, which could be related to increasing the apparent number of electrons (n_{app}). (b) Decreasing of peak C_1 current during the reverse scan, which could indicate that *p*-benzoquinone **1ox** formed at the surface of electrode is removed by chemical reaction with azide ion. In this case, the presence of the cathodic peak C_1 strongly depends on the potential sweep rate. Thus, for the highest sweep rate employed a well-defined cathodic peak C_1 is observed. For lower sweep rates, the peak current ratio (I_{pC1}/I_{pA1}) is less than one. It is about 0.7 for a sweep rate of 10 mV s^{-1}, and it increases when the sweep rate increases. A similar situation is observed when the azide ion to hydroquinone (**1**) concentration ratio is decreased.

Controlled-potential coulometry was performed in aqueous solution containing 0.2 mmol of **1** and 1.5 mmol of azide ion in an undivided cell at 0.2 V (vs SCE). Monitoring of the progress of the electrolysis was carried out by cyclic voltammetry (Fig. 2). As shown, during coulometry, in parallel with the decrease in height of the anodic peak A_1 and its cathodic counterpart (C_1), new anodic (A_2 and A_3), and cathodic counterpart peaks (C_2 and C_3) appear and the height of them increases. At the end of the coulometry all anodic and cathodic peaks disappear and only anodic and cathodic peaks A_3 and C_3 remain. These peaks are related to the redox reaction of **3**/**3ox** couple. The anodic peak A_1 disappears when the charge consumption becomes about 6e^- per molecule of **1**. These observations allow us to propose the pathway (an *ECECE* mechanism) in Scheme 1 for the electrochemical oxidation of **1** in the presence of azide ion. According to our results, it seems that the Michael addition reaction of azide ion to *p*-benzoquinone **1ox** is

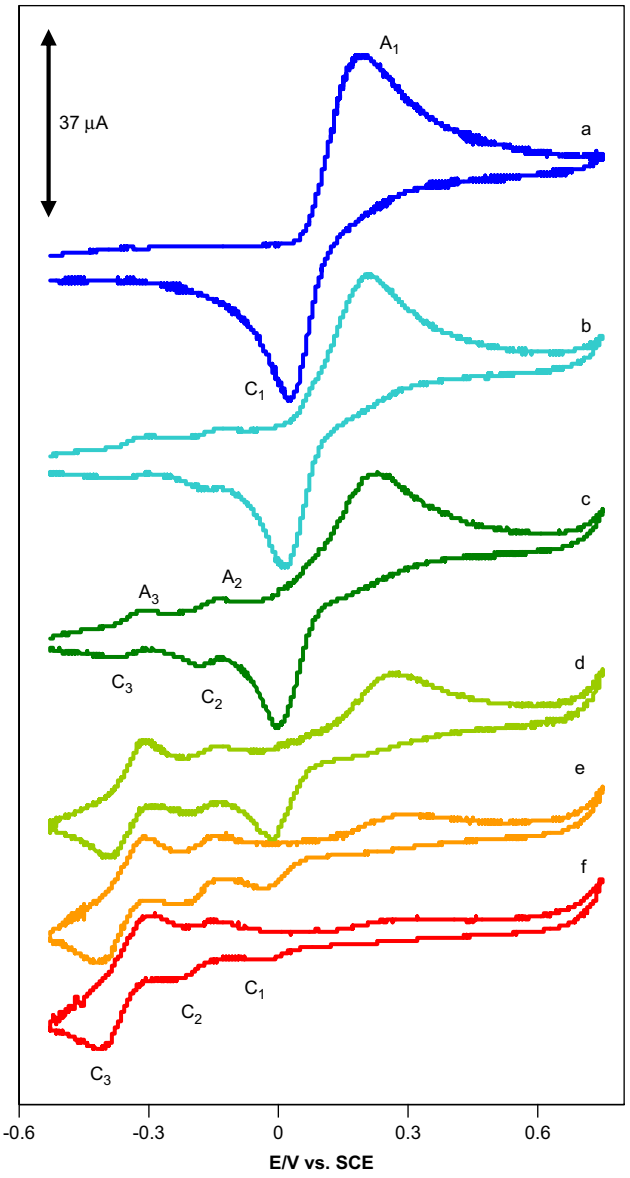

Figure 2. Cyclic voltammograms of 0.2 mmol hydroquinone (**1**) in the presence of 1.5 mmol of azide ion in water containing phosphate buffer (c=0.2 M, pH=6.0) at glassy carbon electrode during controlled-potential coulometry at 0.2 V versus SCE. After consumption of: (a) 0, (b) 15, (c) 30, (d) 60, (e) 100, and (f) 120 C.

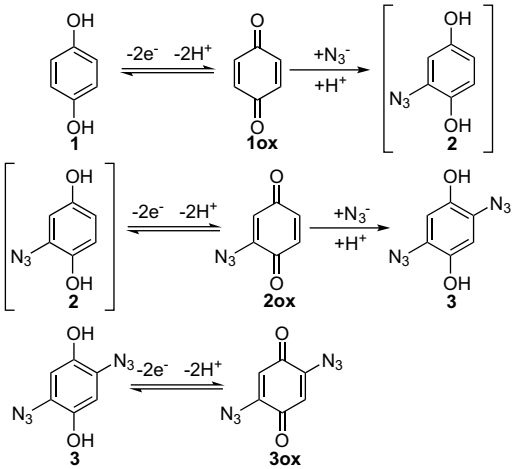

Scheme 1.

faster than other side reactions and leads to azidohydroquinone **2**. The oxidation of compound **2** is easier than the oxidation of hydroquinone **1** by virtue of the presence of an electron-donating group. In the next step, *p*-benzoquinone **2ox**, via a Michael reaction, is converted into diazidohydroquinone **3**. Further oxidation converts diazidohydroquinone **3** into the final product **3ox**.

Accordingly, the anodic peak A_1 pertains to the oxidation of hydroquinone **1** to the *p*-benzoquinone **1ox**. Obviously, the cathodic peak C_1 corresponds to the reduction of the *p*-benzoquinone **1ox**. The new anodic peaks A_2 and A_3 can be related to electrochemical oxidation of azidohydroquinone **2** and diazidohydroquinone **3** to the *p*-benzoquinones **2ox** and **3ox**, respectively. Clearly, the cathodic peaks C_2 and C_3 correspond to the reduction of the *p*-benzoquinones **2ox** and **3ox**, respectively. The presence of electron-donating group(s) on *p*-benzoquinones **2ox** and **3ox** reduces the reactivity of these *p*-benzoquinones toward Michael reactions, so the rate of reactions of these *p*-benzoquinones with azide ions are low and the effects of these reactions are not observed in obtained cyclic voltammograms because of the time scale of the cyclic voltammograms and the times of these chemical reactions are not comparable. However, in controlled-potential coulometry with a longer time scale, the effect of these reactions is observed as an increase in the number of electrons per molecule (n=6) and appearance of new anodic and cathodic peaks (A_2, A_3, C_2, and C_3) in cyclic voltammograms obtained during coulometry (Fig. 2).

2.2. Kinetic evaluation

The electrochemical oxidation of hydroquinone (**1**) in the presence of azide ions was tested by digital simulation. The simulation was carried out assuming semi-infinite one-dimensional diffusion and planar electrode geometry. The experimental parameters entered for digital simulation consisted of the following: E_{start}, E_{switch}, E_{end}, t=25 °C and analytical concentration of hydroquinone (**1**) and azide ion. The transfer coefficient (α) was assumed to be 0.5 and the formal potential was obtained experimentally as the midpoint potential between the anodic and cathodic peaks (E_{mid}). The heterogeneous rate constant (0.002 cm^{-1}) for oxidation of hydroquinone (**1**) was estimated by use of an experimental working curve.[33] All these parameters were kept constant throughout the fitting of the digitally simulated voltammogram to the experimental data. The parameter k_{obs} was allowed to change through the fitting processes. In order to estimation of the observed homogeneous rate constant (k_{obs}) of the reaction of electrochemically generated *p*-benzoquinone **1ox** with azide ion, we studied the electrochemical oxidation of hydroquinone (**1**) in the presence of azide ion at various pHs. The results indicate an increase in anodic peak current A_1 against a decrease in current of cathodic peak C_1, with decreasing pH. As previously reported these observations confirm the homogeneous catalytic pathway for the electrochemical oxidation of **1** in the presence of azide ion in acidic media (Scheme 2).[24] This type of reaction, also previously reported by

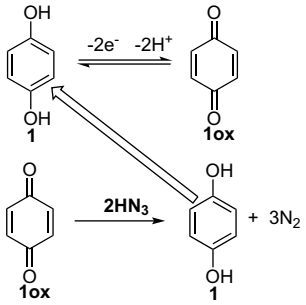

Scheme 2.

Table 1
The calculated k_{obs} based on an *EC′* mechanism for reaction of *p*-benzoquinone **1ox** with azide ion

pH	1.50	1.75	2.00	2.25	2.50
k_{obs} (M^{-1} s^{-1})[a]	1.65±0.18	1.50±0.29	1.36±0.28	1.21±0.25	1.10±0.25

[a] For n=3 at scan rates; 10, 15, and 25 mV s^{-1}.

Couladouros and co-workers in the reaction of hydrazoic acid with naphthoquinone.[1] In this direction, in acidic media, the simulation was performed based on an *EC′* (catalytic) mechanism. The calculated values of the observed homogeneous rate constant (k_{obs}) for reaction of *p*-benzoquinone **1ox** with an azide ion have shown in Table 1.

Figure 3 shows the plot of observed homogeneous rate constant (k_{obs}) as a function of pH. As shown, the k_{obs} decreases linearly with increasing pH and reaches zero at pH=4.5. Here is a competition between catalytic and addition (Michael) reactions. When azide ions are in protonated form (hydrazoic acid, pK_a=4.72[34]) the main reaction is catalytic reaction (Scheme 2), while in less acidic, neutral, and basic solutions, the preferable reaction is Michael addition reaction (Scheme 1). So, for estimation of the observed homogeneous rate constant (k_{obs}) of the reaction of electrochemically generated *p*-benzoquinone **1ox** with azide ion, we simulated cyclic voltammograms of hydroquinone (**1**) (1 mM) in the presence of azide ions (60 mM) at pH=6.0 based on an *ECE* mechanism (Fig. 4). The calculated value of the k_{obs} is 0.21±0.02 M^{-1} s^{-1}.

2.3. Electrochemical oxidation of 2,5-dihydroxybenzoic acid

The electrochemical oxidation of 1 mM solution of 2,5-dihydroxybenzoic acid (**4**) in water containing phosphate buffer (c=0.2 M, pH=6.0) at a bare glassy carbon electrode has been studied using cyclic voltammetry (Fig. 5, curve a). The voltammogram shows one anodic (A_1) and corresponding cathodic peak (C_1), at 0.22 V and 0.16 V versus a standard calomel electrode (SCE), respectively, which corresponds to the transformation of 2,5-dihydroxybenzoic acid (**4**) to *p*-benzoquinone **4ox** and vice versa within a reversible two-electron process (Scheme 3).[26] Figure 5

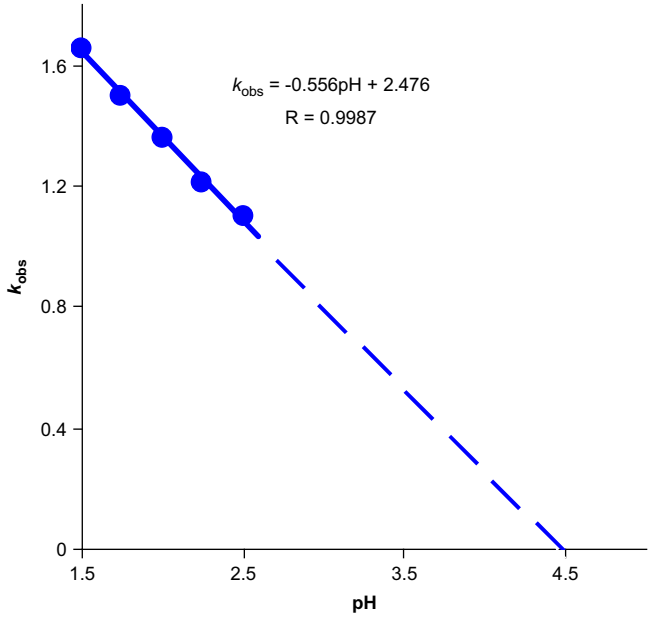

Figure 3. Linear relations between k_{obs} and pH.

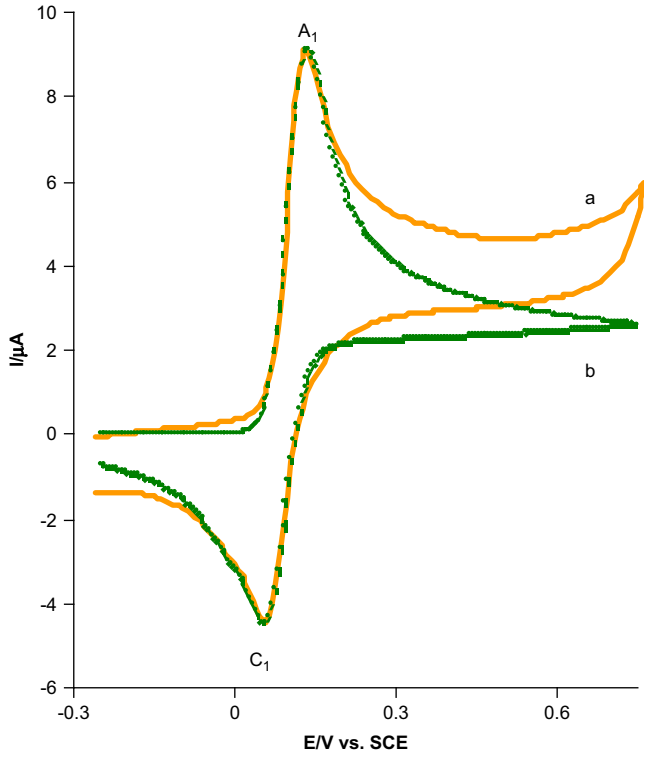

Figure 4. Experimental (curve a) and simulated (curve b) cyclic voltammograms of 1 mM hydroquinone (**1**) in the presence of 60 mM azide ion at glassy carbon electrode, in phosphate buffer solution (c=0.2 M, pH=6.0). Scan rate: 25 mV s^{-1}; t=25±1 °C.

(curves b and c) shows cyclic voltammogram obtained for a 1 mM solution of **4** in the presence of 15 mM azide ion. The voltammogram exhibits two cathodic peaks C_1 (0.16 V vs SCE) and C_2 (0.05 V vs SCE). In the second cycle, a new anodic peak (A_2) appears with an E_p value of 0.10 V versus SCE. The comparison of Figure 5 (curve b) with Figure 1, curve b shows the higher reactivity of Michael acceptor **4ox**, because of the presence of carboxylic acid group as an electron-withdrawn group in structure of **4ox**.

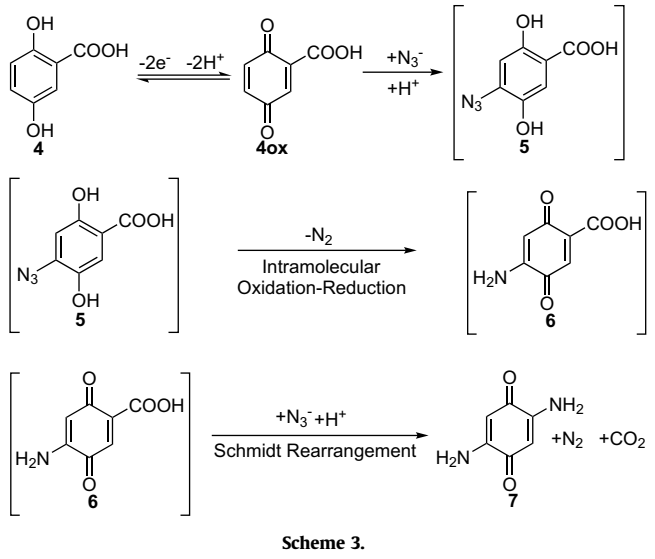

Scheme 3.

Besides, in electrochemical oxidation of 2,5-dihydroxybenzoic acid (**4**) in the presence of azide ion, proportional to the increasing of the potential sweep rate and in parallel with the decrease in current of C_2, the current of C_1 increases (Fig. 6). Under these conditions, the peak current ratios (I_{pC1}/I_{pA1}) and (I_{pC2}/I_{pC1}) versus scan rate for a mixture of 2,5-dihydroxybenzoic acid (**4**) and azide ion shows the reactivity of **4ox** toward azide ion, appearing as an increase in the peak current ratio I_{pC1}/I_{pA1} and decrease in the peak current ratio I_{pC2}/I_{pC1} at higher scan rates. A comparable condition is observed when the azide ion to **4ox** concentration ratio is decreased. Also, under these conditions, the current function for peak A_1 ($I_{pA1}/v^{1/2}$) decreases with increasing scan rate. According to the obtained electrochemical data and the spectroscopic data of the final product, we propose the mechanism shown in Scheme 3 for the electrochemical oxidation of **4** in the presence of azide ions.

According to our results, the Michael addition reaction of azide ion to *p*-benzoquinone **4ox** leads to azidohydroquinone **5**. In the

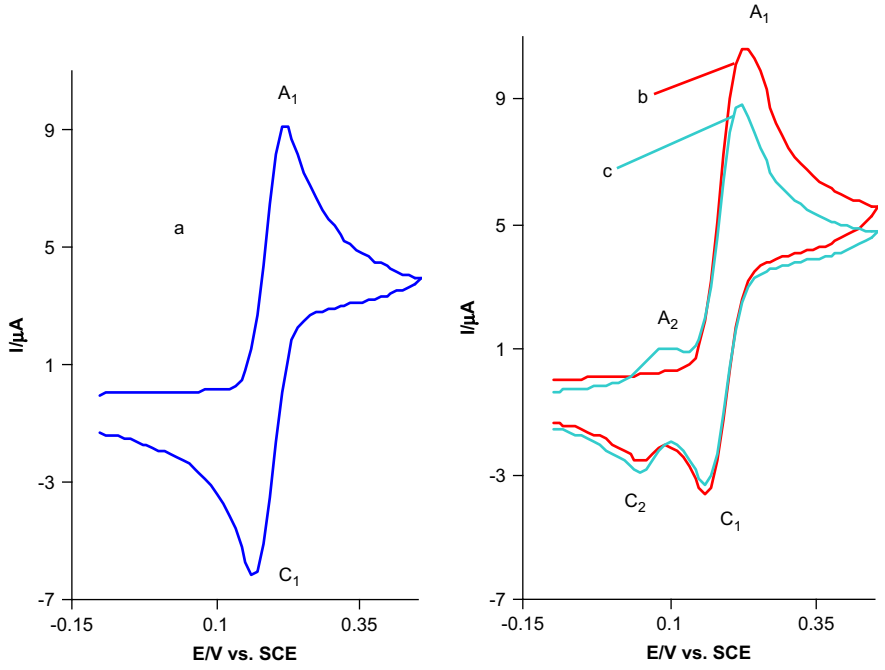

Figure 5. Cyclic voltammograms of: (a) 1 mM 2,5-dihydroxybenzoic acid (**4**), (b) and (c) first and second cycles of 1 mM 2,5-dihydroxybenzoic acid (**4**) in the presence of 15 mM azide ion, respectively, at glassy carbon electrode, in aqueous solution containing 0.2 M phosphate buffer (pH 6.0). Scan rate: 25 mV s^{-1}; t=25±1 °C.

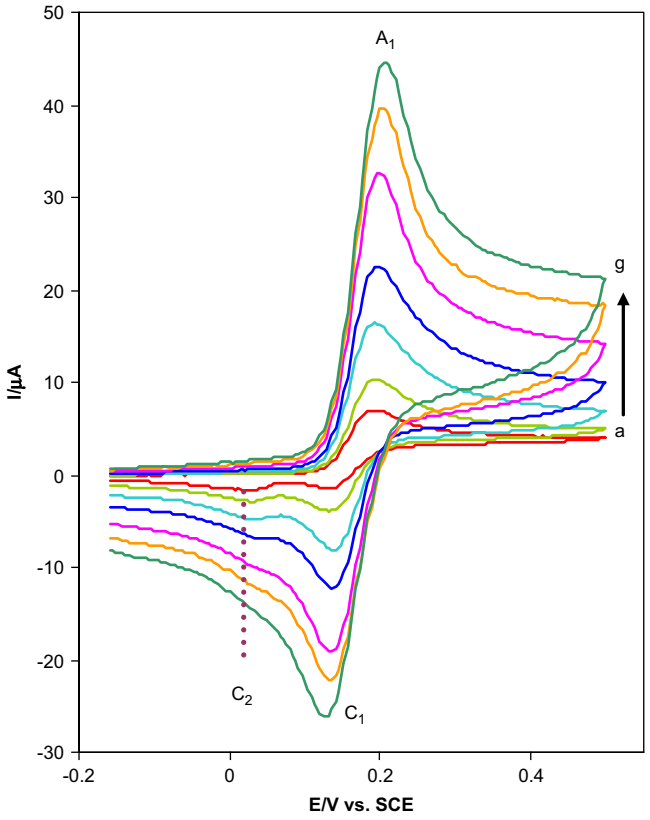

Figure 6. Typical cyclic voltammograms of 1 mM 2,5-dihydroxybenzoic acid (**4**) in the presence of 15 mM azide ion at a glassy carbon electrode, in aqueous solution containing 0.2 M phosphate buffer (pH 6.0). Scan rates from (a) to (g) are: 10, 25, 50, 100, 200, 300, and 400 mV s^{-1}, respectively. t=25±1 °C.

next step, azidohydroquinone **5**, via an overall intramolecular oxidation–reduction reaction,[1] converts into amino-*p*-benzoquinone **6**. Next addition of azide ion and Schmidt rearrangement[35] converts **6** into diamino-*p*-benzoquinone **7** as the final product. Consequently, the anodic peak A_1 pertains to the oxidation of **4** to the *p*-benzoquinone **4ox**. Clearly, peak C_1 corresponds to the reduction of **4ox**. The new anodic peak A_2 can be related to oxidation of **5** to *p*-benzoquinone **5ox** and the cathodic peak C_2 is counterpart of it. Since the rate of intramolecular oxidation–reduction reaction and Schmidt reaction are slow, the effects of these reactions are not observed in the time scale of the cyclic voltammograms.

Formation of amino-*p*-benzoquinone **6** under intramolecular oxidation–reduction reaction conditions can be rationalized as shown in Scheme 4. According to this mechanism, **5c** is converted into **5d** by loss of N_2. Compound **5d** is then readily transformed into the stable tautomeric form **6**.

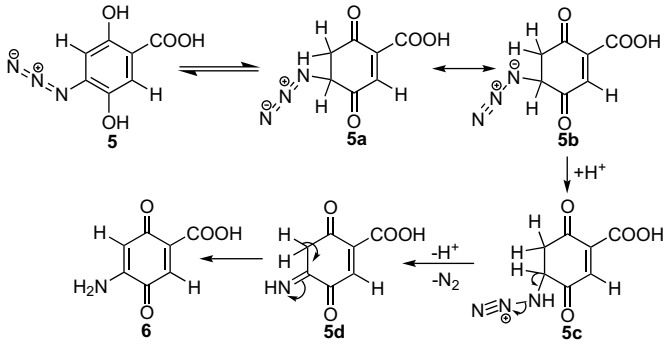

Scheme 4.

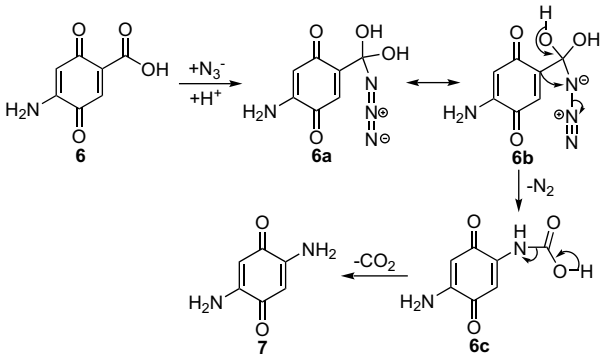

Scheme 5.

The formation of diamino-*p*-benzoquinone **7** via Schmidt rearrangement[2,35,36] is showed in Scheme 5.

The difference in behavior of electrochemical oxidation of hydroquinone (**1**) and 2,5-dihydroxybenzoic acid (**4**) in the presence of azide ion can be attributed to (1) the enol–keto equilibrium in the case of **5** (in comparison with **2**) arising from intramolecular hydrogen bonding (Scheme 6), (2) the easy loss of dinitrogen from the **5c** due to the more electron-withdrawing character of *para*-quinone ring because of the presence of the carboxyl group with electro-withdrawing character. In other words, it seems that electro-withdrawing group, i.e., –COOH in benzene ring makes $-N_3$ group more easier to mediate intramolecular oxidation–reduction to form $-NH_2$, compared to hydroquinone where final product is diazidohydroquinone rather than diaminohydroquinone.

For estimation of the observed homogeneous rate constant (k_{obs}) of the reaction of electrochemically generated *p*-benzoquinone **4ox** with azide ion, we simulated cyclic voltammograms of 2,5-dihydroxybenzoic acid (**4**) (1 mM) in the presence of azide ions (15 mM) at pH=6.0, based on an *ECE* mechanism (Fig. 7). The calculated value of the k_{obs} is 1.93±0.05 M^{-1} s^{-1}. The comparison of this number with the observed homogeneous rate constant (k_{obs}) of hydroquinone (**1**) (0.21±0.02), shows the presence of electron-withdrawing carboxylic group on the hydroquinone ring causes an increase in k_{obs}.

2.4. Electrochemical oxidation of 3,4-dihydroxybenzoic acid

The cyclic voltammogram of a 1 mM solution of 3,4-dihydroxybenzoic acid (**8**) in aqueous solution containing 0.2 M phosphate buffer (pH 6.0) is shown in Figure 8 (curve a). The voltammogram shows one anodic (A_1) and a corresponding cathodic peak (C_1), which corresponds to the transformation of 3,4-dihydroxybenzoic acid (**8**) to *o*-benzoquinone **8ox** and vice versa within a quasi-reversible two-electron process.[26,28] Figure 8 (curve b) shows the cyclic voltammogram obtained for a 1 mM solution of **8** in the presence of 15 mM azide ion in same condition. The voltammogram exhibits one anodic peak A_1 and three cathodic peaks (C_1, C_2, and C_3). In the second cycle, the voltammogram shows that, parallel to the decrease in current of A_1 and the shift of its potential in a positive direction, two new anodic peaks (A_2 and A_3) appear at less positive potentials (Fig. 8 (curve c)).

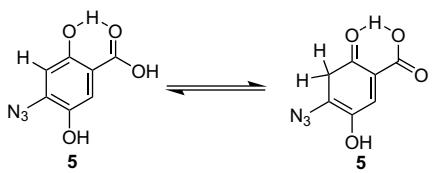

Scheme 6.

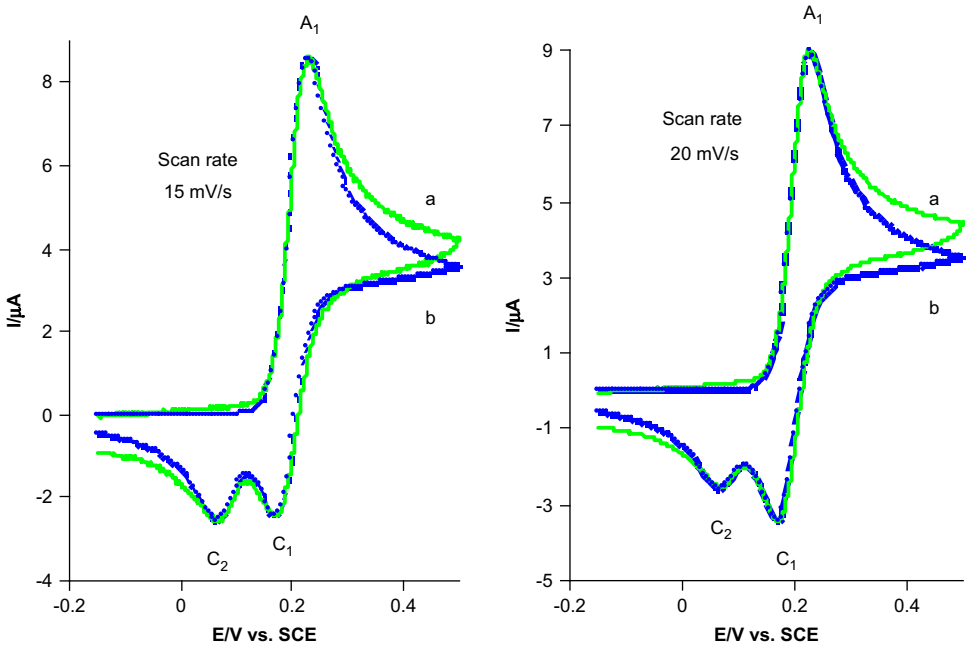

Figure 7. Experimental (curves a) and simulated (curves b) cyclic voltammograms of 1 mM 2,5-dihydroxybenzoic acid (**4**) in the presence of 15 mM azide ion at glassy carbon electrode, in phosphate buffer solution (c=0.2 M, pH=6.0). Scan rate: 15 and 20 mV s^{-1}; t=25±1 °C.

The positive shift of the peak A_1 in the presence of azide ion is due to the formation of a thin film of product at the surface of the electrode, inhibiting to a certain extent, the performance of the electrode process. Also, it is seen that proportional to the increasing of the potential sweep rate, parallel to the increase in height of the C_1 the height of C_2 and C_3 decreases (Fig. 9). A similar situation is observed when the azide ion to **8** concentration ratio is decreased. According to these data and the spectroscopic data of the final product, which is as same as obtained product in electrochemical oxidation of catechol in the presence of azide ions,[24] we propose the mechanism shown in Scheme 7 for the electrochemical oxidation of **8** in the presence of azide ions.

According to proposed mechanism, the anodic peak A_1 pertains to the oxidation of **8** to the *o*-benzoquinone **8ox** and cathodic peak C_1 is its counterpart. The new anodic peaks A_2 and A_3 can be related to electrochemical oxidation of **9** (to **9ox**) and **10red**, respectively. Intermediates **9ox** and **10red** are anodic and cathodic counterparts of **9** and **10**, respectively. Clearly, the cathodic peaks C_2 and C_3

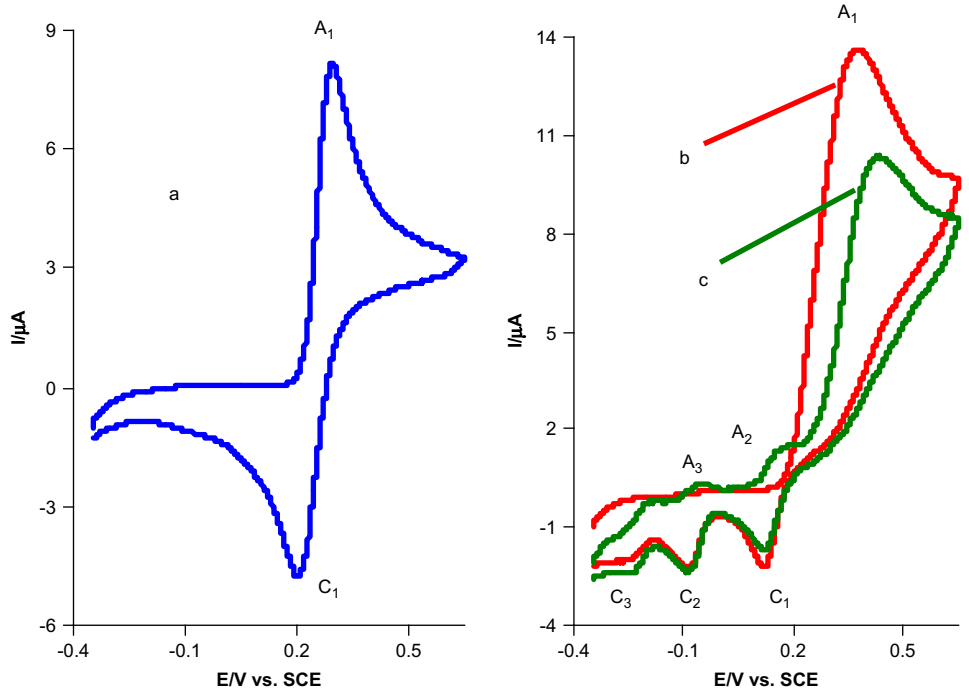

Figure 8. Cyclic voltammograms of: (a) 1 mM 3,4-dihydroxybenzoic acid (**8**), (b) and (c) first and second cycles of 1 mM 3,4-dihydroxybenzoic acid (**8**) in the presence of 15 mM azide ion, respectively, at glassy carbon electrode, in aqueous solution containing 0.2 M phosphate buffer (pH 6.0). Scan rate: 25 mV s^{-1}; t=25±1 °C.

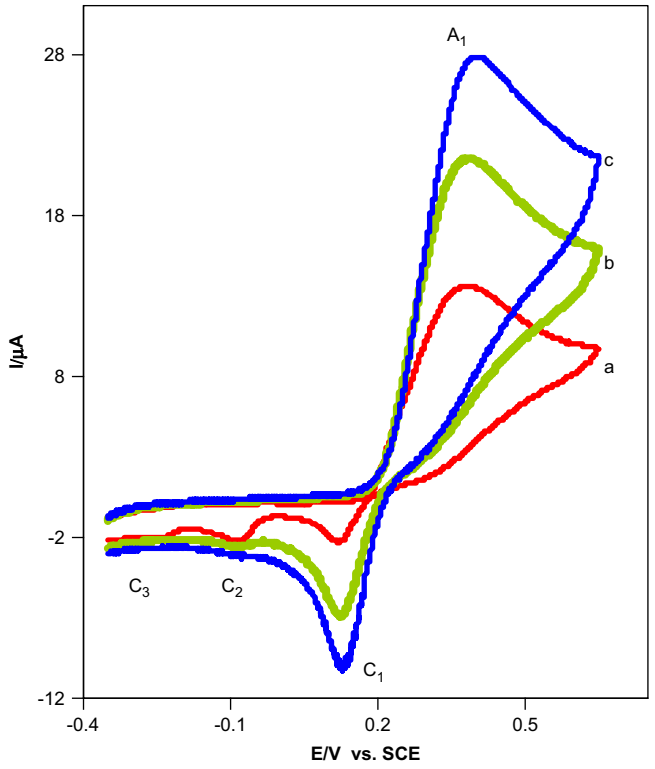

Figure 9. Typical cyclic voltammograms of 1 mM 3,4-dihydroxybenzoic acid (**8**) in the presence of 15 mM azide ion at a glassy carbon electrode, in aqueous solution containing 0.2 M phosphate buffer (pH 6.0). Scan rates from (a) to (c) are: 25, 100, and 200 mV s^{-1}, respectively. t=25±1 °C.

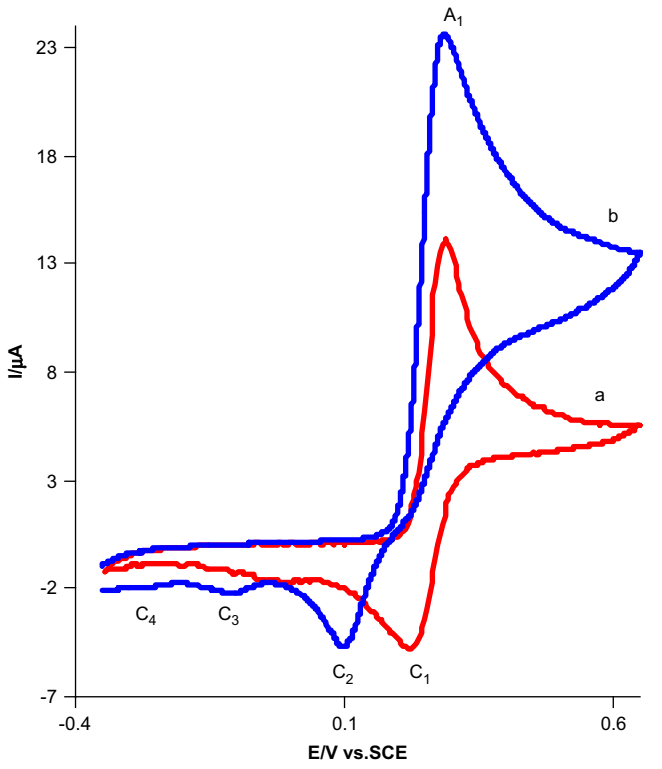

Figure 10. Cyclic voltammograms of 1 mM 2,3-dihydroxybenzoic acid (**12**): (a) in the absence of azide ion, (b) in the presence of 15 mM of azide ion, at a glassy carbon electrode, in aqueous solution containing 0.2 M phosphate buffer (pH 6.0). Scan rate: 25 mV s^{-1}; t=25±1 °C.

correspond to the reduction of the *o*-benzoquinones **9ox** and **10**, respectively. Because, the rate of Schmidt reaction is slow, the effect of it is not observed in the time scale of the cyclic voltammograms.

The comparison of Figure 8 (curve b) with Figure 5, curve b shows the higher reactivity of Michael acceptor **8ox**, due to the more reactivity of *ortho*-quinone ring in comparison with *para*-quinone ring.

2.5. Electrochemical oxidation of 2,3-dihydroxybenzoic acid

Cyclic voltammograms of 2,3-dihydroxybenzoic acid (**12**) in the absence and in the presence of azide ion in water containing phosphate buffer (c=0.2 M, pH=6.0) at a bare glassy carbon electrode are shown in Figure 10. The cyclic voltammogram of **12** in the absence of azide ion (curve a) shows one anodic peak (A_1) at 0.29 V and the corresponding cathodic peak (C_1) at 0.22 V, which corresponds to the transformation of 2,3-dihydroxybenzoic acid (**12**) into the related *o*-benzoquinone (5,6-dioxocyclohexa-1,3-dienecarboxylic acid, **12ox**) and vice versa within a quasi-reversible two-electron process.[28] Figure 10 (curve b) shows the cyclic voltammogram obtained for a 1 mM solution of **12** in the presence of 15 mM azide ion at 25 mV s^{-1}. The voltammogram exhibits three cathodic peaks C_2 (0.09 V vs SCE), C_3 (−0.12 V vs SCE) and C_4 (−0.28 V vs SCE). For more data, the influence of the potential sweep rate on the shape of cyclic voltammograms of a solution of **12** in the presence of azide ion has been studied (Fig. 11). The results show that proportional to the increasing of the potential sweep rate, in the beginning, the cathodic peaks C_4 and C_3 disappears (curves a and b) and then the cathodic peak C_1 appears and in parallel with the decrease in current of C_2, the height of it increases (Fig. 11 curves c–f). A comparable condition is observed when the azide ion to **12** concentration ratio is decreased. These voltammetric data in addition to spectroscopic data (IR, ^{1}H NMR, ^{13}C NMR, and MS) of the final product cause us to propose the following mechanism for electrochemical oxidation of 2,3-dihydroxybenzoic acid (**12**) in the presence of azide ions (Scheme 8).

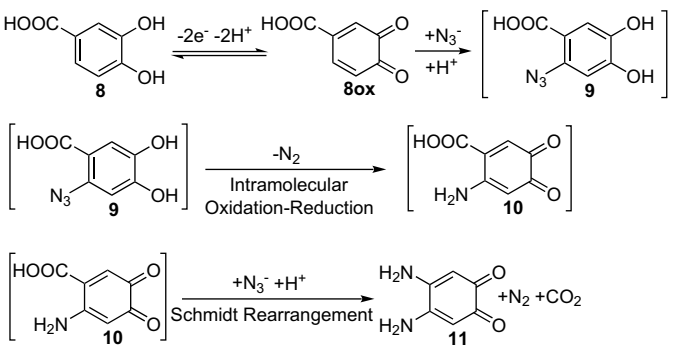

Scheme 7.

According to the proposed mechanism, the cathodic peaks C_1, C_2, C_3, and C_4 can be related to the reduction of intermediates **12ox**, **13ox** (counterpart of **13**), **14**, and **15ox** (counterpart of **15**), respectively.

3. Conclusions

The present results complete the previous reports on the anodic oxidation of catechol in the presence of azide ion.[24] In this report, the mechanism of the reaction of electrochemically generated *para* and *ortho*-benzoquinones with azide ions is investigated, and a method of general applicability for their high-yield synthesis under mild experimental conditions is provided.

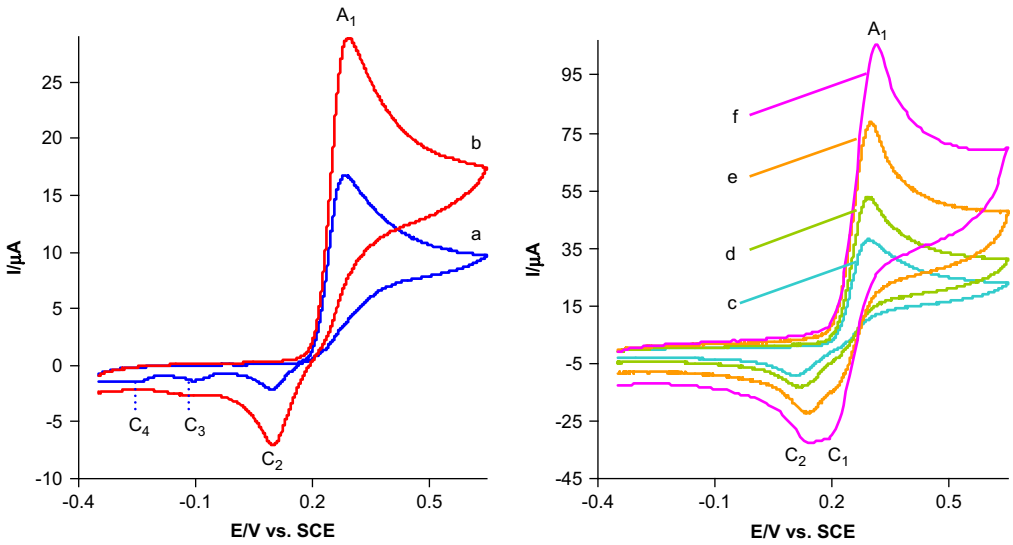

Figure 11. Typical cyclic voltammograms of 1 mM 2,3-dihydroxybenzoic acid (**12**) in the presence of 15 mM azide ion at a glassy carbon electrode, in aqueous solution containing 0.2 M phosphate buffer (pH 6.0). Scan rates from (a) to (f) are: 10, 50, 100, 200, 400, and 1000 mV s^{-1}, respectively. t=25±1 °C.

We observed an interesting diversity in the mechanism of electrochemical oxidation of hydroquinone (**1**) and other *para* and *ortho* dihydroxybenzoic acid derivatives (**4**, **8**, and **12**) in the presence of azide ion. In the case of hydroquinone (**1**), the final product is diazido-*p*-benzoquinone **3ox**, whereas in the cases of 2,5-dihydroxybenzoic acid (**4**) and 3,4-dihydroxybenzoic acid (**8**), the final products (**7** and **11**) are diaminobenzoquinones that were obtained after intermolecular Michael addition reaction, intramolecular oxidation–reduction and Schmidt reactions. Also, in the case of 2,3-dihydroxybenzoic acid (**12**), the final product, which is diamino-*o*-benzoquinone **16**, was obtained after two successive intermolecular Michael addition reactions and intramolecular oxidation–reduction. The difference in behavior of electrochemical oxidation of hydroquinone (**1**) with other *para* and *ortho* dihydroxybenzoic acid derivatives (**4**, **8**, and **12**) in the presence of azide ion is attributed to the enol–keto equilibrium due to intramolecular hydrogen bonding as well as the easy loss of dinitrogen due to the more electron-withdrawing character of *para* (because of the presence of carboxyl group) and *ortho*-quinone rings. Finally, we can state that the addition of azide anion to hydroquinone (**1**) and other *para* and *ortho* dihydroxybenzoic acid derivatives (**4**, **8**, and **12**) is an interesting reaction that provides direct access to diazido-*p*-benzoquinone and diaminobenzoquinones, respectively.

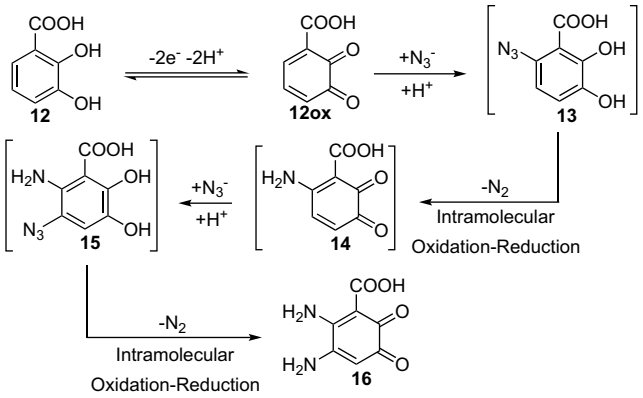

Scheme 8.

4. Experimental

4.1. Electrodes, electrochemical instruments, and chemicals

Cyclic voltammetry, controlled-potential coulometry and preparative electrolysis were performed using a Behpajoh model BHP-2062 potentiostat/galvanostat. The working electrode used in the voltammetry experiments was a glassy carbon disc (1.8 mm^2 area) and platinum wire was used as a counter electrode. The working electrode used in controlled-potential coulometry and macroscale electrolysis was an assembly of four graphite rods (31 cm^2) and a large stain less steely gauze constitutes the counter electrode. The working electrode potentials were measured versus SCE (all electrodes from AZAR electrode). Hydroquinone, 2,5-dihydroxybenzoic acid, 3,4-dihydroxybenzoic acid, and 2,3-dihydroxybenzoic acid were reagent-grade materials from Aldrich and sodium azide, phosphoric acid, acetic acid, ammonia, etc. were of pro-analysis grade from E. Merck. These chemicals were used without further purification. The homogeneous rate constants were estimated by analyzing the cyclic voltammetric responses, using the DigiElch simulation software.[37] An excellent fit between the experimental and simulated data was obtained over this range of experimental conditions for the following kinetic parameter values.

4.2. Electroorganic synthesis of 3ox, 7, 11, and 16

A solution (ca. 80 mL) of aqueous phosphate buffer solution (c=0.2, pH 6.0) containing 3 mmol of hydroquinone (or 2,5-dihydroxybenzoic acid, 3,4-dihydroxybenzoic acid, 2,3-dihydroxybenzoic acid) and 20 mmol of sodium azide was electrolyzed at potential of peak A_1 in an undivided cell equipped with a carbon anode and a large stain less steely gauze as cathode, at 25 °C. The electrolysis was terminated when the current decayed to 5% of its original value. The process was interrupted during the electrolysis and the carbon anode was washed in acetone in order to reactivate it. For the synthesis of **3ox**, **7**, and **11** at the end of electrolysis, cell was placed in refrigerator overnight. The solid precipitated was collected by filtration and was washed several times with water. The synthesis of **16** performed under similar conditions as for the **3ox**, **7**, and **11**, but at the end of electrolysis, after evaporation of solvent, the product was purified by column chromatography (silica

gel, dichloromethane/ethanol (80:20)). The isolated yields of **3ox**, **7**, **11**, and **16** are 67%, 71%, 73%, and 70%, respectively.

4.3. Characteristics of products

*4.3.1. 2,5-Diazido-1,4-benzoquinone (**3ox**)*

The product **3ox** was obtained as orange precipitate, (67% yield), mp 96–68 °C (dec) (lit. 93–94[13]). IR (Nujol) 2137 and 2093 (azide), 1651 (quinone carbonyl), 1573, 1463, 1377, 1277, 1213, 868, 761, 722 cm^{-1}; ^1H NMR (acetone-d_6, 90 MHz): δ 6.28 (s); ^{13}C NMR (acetone-d_6, 22.5 MHz): δ 116.0, 146.1, 181.5.

*4.3.2. 2,5-Diamino-1,4-benzoquinone (**7**)*

The product **7** was obtained as purple precipitate, (71% yield), mp >380 °C. IR (KBr) 3352, 3120, 1663, 1534, 1418, 1257, 1061, 843, 749, 681 cm^{-1}; ^1H NMR (DMSO-d_6, 90 MHz): δ 5.32 (s, 2H), 7.32 (br 4H); ^{13}C NMR (DMSO-d_6, 75 MHz): δ 116.1, 150.2, 178.5. MS (*m*/*z*) (relative intensity) 138 ($M^{+\bullet}$, 100), 111 (16), 70 (19).

*4.3.3. 4,5-Diamino-1,2-benzoquinone (**11**)*

The product **11** was obtained as violet precipitate, (73% yield), mp >300 °C (lit. >300 °C[24]). IR (KBr) 3431, 3066, 1722, 1684, 1577, 1532, 1465, 1294, 831, 670 cm^{-1}; ^1H NMR (DMSO-d_6, 90 MHz): δ 5.32 (s, 2H), 7.44 (br 4H); ^{13}C NMR (DMSO-d_6, 22.5 MHz): δ 98.6, 153.4, 178.8.

*4.3.4. 2,3-Diamino-5,6-dioxocyclohexa-1,3-dienecarboxylic acid (**16**)*

The product **16** was obtained as dark violet precipitate, (70% yield), mp >350 °C. IR (KBr) 3179, 1680, 1623, 1558, 1470, 1406, 1113, 822, 701 cm^{-1}; ^1H NMR (DMSO-d_6, 90 MHz): δ 5.63 (s, 1H), 7.77 (br 2H, this peak disappears in the presence of D_2O), 9.5 (br about 2H, this peak disappears in the presence of D_2O), 11.16 (br 1H, this peak disappears in the presence of D_2O); ^{13}C NMR (DMSO-d_6, 22.5 MHz): δ 96.6, 102.2, 150.9, 160.7, 169.7, 176.7, 179.1. MS (*m*/*z*) (relative intensity) 182 ($M^{+\bullet}$, 1.5), 138 (3.9), 135 (5.2), 68 (100).

Acknowledgements

We would like to thank Dr. M. Rudolph for his cyclic voltammogram digital simulation software (DigiElch SB) and the authors acknowledge the Bu-Ali Sina University Research Council and Center of Excellence in Development of Chemical Methods (CEDCM) for support this work.

References and notes

1. Couladouros, E. A.; Plyta, Z. F.; Haroutounian, S. A.; Papageorgiou, V. P. *J. Org. Chem.* **1997**, *62*, 6.
2. Scriven, E. F.; Turnbull, K. *Chem. Rev.* **1988**, *88*, 297.
3. Labbe, G. *Chem. Rev.* **1968**, *69*, 345.
4. Weyler, W.; Pearce, D. S., Jr.; Moore, H. W. *J. Am. Chem. Soc.* **1973**, *95*, 2603.
5. Moore, H. W.; Decker, O. H. W. *Chem. Rev.* **1986**, *86*, 821.
6. Germeraad, P.; Moore, H. W. *J. Org. Chern.* **1974**, *39*, 774.
7. Weyler, W.; Duncan, W. G., Jr.; Moore, H. W. *J. Am. Chem. Soc.* **1975**, *97*, 6178.
8. Pearce, D. S., Jr.; Locke, M. J.; Moore, H. W. *J. Am. Chem. Soc.* **1975**, *97*, 6181.
9. Germeraad, P.; Weyler, W., Jr.; Moore, H. W. *J. Org. Chem.* **1974**, *39*, 781.
10. Cajipe, G. J. B.; Landen, G.; Semler, B.; Moore, H. W. *J. Org. Chem.* **1975**, *40*, 3874.
11. Naruta, Y.; Nagai, N.; Arita, Y.; Maruyama, K. *J. Org. Chem.* **1987**, *52*, 3956.
12. Chow, K.; Moore, H. W. *J. Org. Chem.* **1990**, *55*, 370.
13. Moore, H. W.; Shelden, H. R.; Shellhamer, D. F. *J. Org. Chem.* **1969**, *34*, 1999.
14. Moore, H. W.; Shelden, H. R.; Deters, D. W.; Wikholm, R. J. *J. Am. Chem. Soc.* **1970**, *92*, 1675.
15. Boger, D. L.; Duff, S. R.; Panek, J. S.; Yasuda, M. J. *J. Org. Chem.* **1985**, *50*, 5782.
16. Boger, D. L.; Duff, S. R.; Panek, J. S.; Yasuda, M. J. *J. Org. Chem.* **1985**, *50*, 5790.
17. Renault, J.; Giorgi-Renault, S.; Baron, M.; Mailliet, P.; Paoletti, C.; Cros, S.; Voisin, E. J. *J. Med. Chem.* **1983**, *26*, 1715.
18. Kende, S.; Ebetino, F. H. *Tetrahedron Lett.* **1984**, *25*, 923.
19. Nagaoka, H.; Kishi, Y. *Tetrahedron* **1981**, *37*, 3873.
20. Thomson, R. H. *Naturally Occurring Quinones*, 2nd ed.; Academic: New York, NY, 1971.
21. Lancini, G.; Zanichelli, W. In *Antibiotics*; Perlman, D., Ed.; Academic: New York, NY, 1971; pp 531–600.
22. Lin, T. S.; Xu, S. P.; Zhu, L. Y.; Divo, A.; Sartorelli, A. *J. Med. Chem.* **1991**, *34*, 1634.
23. Huang, Z. D.; Chen, Y. N.; Menon, K.; Teicher, B. A. *J. Med. Chem.* **1993**, *36*, 1797.
24. Nematollahi, D.; Afkhami, A.; Tammari, E.; Shariatmanesh, T.; Hesari, M.; Shojaeifard, M. *Chem. Commun.* **2007**, 162.
25. Nematollahi, D.; Tammari, E. *J. Org. Chem.* **2005**, *70*, 7769.
26. Nematollahi, D.; Rafiee, M. *Green Chem.* **2005**, *7*, 638.
27. Nematollahi, D.; Habbibi, D.; Rahmati, M.; Rafiee, M. *J. Org. Chem.* **2004**, *69*, 2637.
28. Nematollahi, D.; Goodarzi, H. *J. Org. Chem.* **2002**, *67*, 5036.
29. Hosseiny Davarani, S. S.; Nematollahi, D.; Mashkouri Najafi, N.; Masoumi, L.; Ramyar, S. *J. Org. Chem.* **2006**, *71*, 2139.
30. Nematollahi, D.; Workentin, M. S.; Tammari, E. *Chem. Commun.* **2006**, 1631.
31. Nematollahi, D.; Amani, A.; Tammari, E. *J. Org. Chem.* **2007**, *72*, 3646.
32. Nematollahi, D.; Shayani-jam, H. *J. Org. Chem.* **2008**, *73*, 3428.
33. Greef, R.; Peat, R.; Peter, L. M.; Pletcher, D.; Robinson, J. *Instrumental Methods in Electrochemistry*; Ellis Horwood: New York, NY, 1990; p 189.
34. Bjerrum, J.; Schwarzenbach, G.; Sillen, L. G. *Stability Constants of Metal-ion Complexes*; Chemical Society: London, 1958.
35. Schmidt, K. F. *Ber.* **1924**, *57*, 704.
36. Patai, S. *The Chemistry of the Azido Group*; Wiley: New York, NY, 1971.
37. Rudolph, M. *J. Electroanal. Chem.* **2002**, *529*, 97 Also, see: http://www.digielch.de.